

Discontinuous phase transition in an annealed multi-state majority-vote model

Guofeng Li¹, Hanshuang Chen^{1,*}, Feng Huang², and Chuansheng Shen^{3,4}

¹*School of Physics and Materials Science,
Anhui University, Hefei, 230601, China*

²*School of Mathematics and Physics,
Anhui Jianzhu University, Hefei 230601, China*

³*Department of Physics, Humboldt University, 12489 Berlin, Germany*

⁴*Department of Physics, Anqing Normal University, Anqing, 246011, China*

(Dated: July 5, 2018)

Abstract

In this paper, we generalize the original majority-vote (MV) model with noise from two states to arbitrary q states, where q is an integer no less than two. The main emphasis is paid to the comparison on the nature of phase transitions between the two-state MV (MV2) model and the three-state MV (MV3) model. By extensive Monte Carlo simulation and mean-field analysis, we find that the MV3 model undergoes a discontinuous order-disorder phase transition, in contrast to a continuous phase transition in the MV2 model. A central feature of such a discontinuous transition is a strong hysteresis behavior as noise intensity goes forward and backward. Within the hysteresis region, the disordered phase and ordered phase are coexisting.

PACS numbers: 89.75.Hc, 05.45.-a, 64.60.Cn

*Electronic address: chenhsf@ahu.edu.cn

I. INTRODUCTION

Spin models like Ising model play a fundamental role in studying phase transitions and critical phenomena in the field of statistical physics and many other disciplines [1]. They have also significant implications for understanding social phenomena where co-ordination dynamics is observed, e.g., in consensus formation and adoption of innovations [2]. The spin orientations can represent the choices made by an agent on the basis of information about its local neighborhood.

The two-state majority-vote (MV2) model with noise, proposed by Oliveira in 1992 [3], is one of the simplest nonequilibrium generalizations of the Ising model. The model presents up-down symmetry and a continuous order-disorder phase transition at a critical value of noise. Studies on regular lattices showed the critical exponents are the same as those of the Ising model [3–7], in accordance with the conjecture by Grinstein *et al.* [8]. The MV2 model has also been extensively studied in complex networks, including random graphs [9, 10], small world networks [11–13], scale-free networks [14–16], and some others [17, 18]. These studies have shown that MV2 models defined on different complex networks belong to different universality classes and the critical exponents depend on the topology of the network topologies. The generalization to a three-state majority-vote model (MV3) on a regular lattice was considered by [19, 20], where the authors found the critical exponents for this non-equilibrium MV3 model are in agreement with the ones for the equilibrium three-states Potts model [21], supporting again the conjecture of [8]. Recently, Melo *et al.* studied the MV3 model on random graphs and they found that the critical noise is a function of the mean connectivity of the graph [22]. In [23], Lima introduced a new zero-state to MV2 model in square lattices and found that this model also falls into the Ising universality. Costa *et al.* generalized the state variable of the MV model from discrete case to continuous one, and they found that a Kosterlitz-Thouless-like phase appears in low values of noise [24].

In the present work, we generalize the MV model to arbitrary multiple states where each agent is allowed to be in one of q different states with q being an integer no less than two. In each step, an agent is randomly chosen and assumes that its state aligns with the state of the majority of its neighborhood with probability $1 - f$ and with the minority state with probability f . Herein, the number of neighboring spins of any agent is fixed that randomly selected from all the other agents at each step. We mainly focus on the difference in the

nature of the order-disorder phase transition between the MV2 model and the MV3 model. Interestingly, we find that in the MV3 model there exists a strong hysteresis behavior as noise intensity goes forward and backward, the main feature of a discontinuous phase transition, in contrast to a continuous phase transition in the MV2 model. A mean-field theory is used to explain the nature of this phase transition.

II. MODEL

Here, we generalize the original MV model from two states to arbitrary multiple states. The model is defined as follows. Each agent i ($= 1, \dots, N$) can be in any one of q states: $\sigma_i \in \{1, \dots, q\}$. The number of the neighboring agents of agent i in any state α can be calculated as $n_\alpha = \sum_{j \in \mathcal{N}(i)} \delta_{\alpha, \sigma_j}$, where the summation takes over all neighboring nodes of i . $\delta_{\alpha, \beta}$ is Kronecker symbol defined as $\delta_{\alpha, \beta} = 1$ if $\alpha = \beta$ and $\delta_{\alpha, \beta} = 0$ otherwise. With the probability $1 - f$, the agent i take the same value as the majority spin, i.e., $\sigma_i = \alpha|_{n_\alpha = \max\{n_1, \dots, n_q\}}$. With the supplementary probability f the agent i takes the same value as the minority spin, i.e., $\sigma_i = \alpha|_{n_\alpha = \min\{n_1, \dots, n_q\}}$. If there are more than two possible states in the majority spin or in the minority spin, we randomly choose one of them. If $q = 2$, we recover the original MV2 model. In the present work, we consider the model defined on random degree-regular networks with annealed randomness, i.e., the number of neighbors of each agent is fixed but they are randomly chosen from all others at each time step.

To characterize the critical behavior of the model, we define the order parameter as

$$m = \left| N^{-1} \sum_{j=1}^N e^{I2\pi\sigma_j/q} \right| \quad (1)$$

where I is the imaginary unit. $m > 0$ corresponds to an ordered state, and $m = 0$ to a disordered state. Furthermore, we define the susceptibility χ and Binder's fourth-order cumulant U as

$$\chi = N [\langle m^2 \rangle - \langle m \rangle^2] \quad (2)$$

$$U = 1 - \frac{\langle m^4 \rangle}{3\langle m^2 \rangle^2} \quad (3)$$

where $\langle \dots \rangle$ denotes time averages taken in the stationary regime.

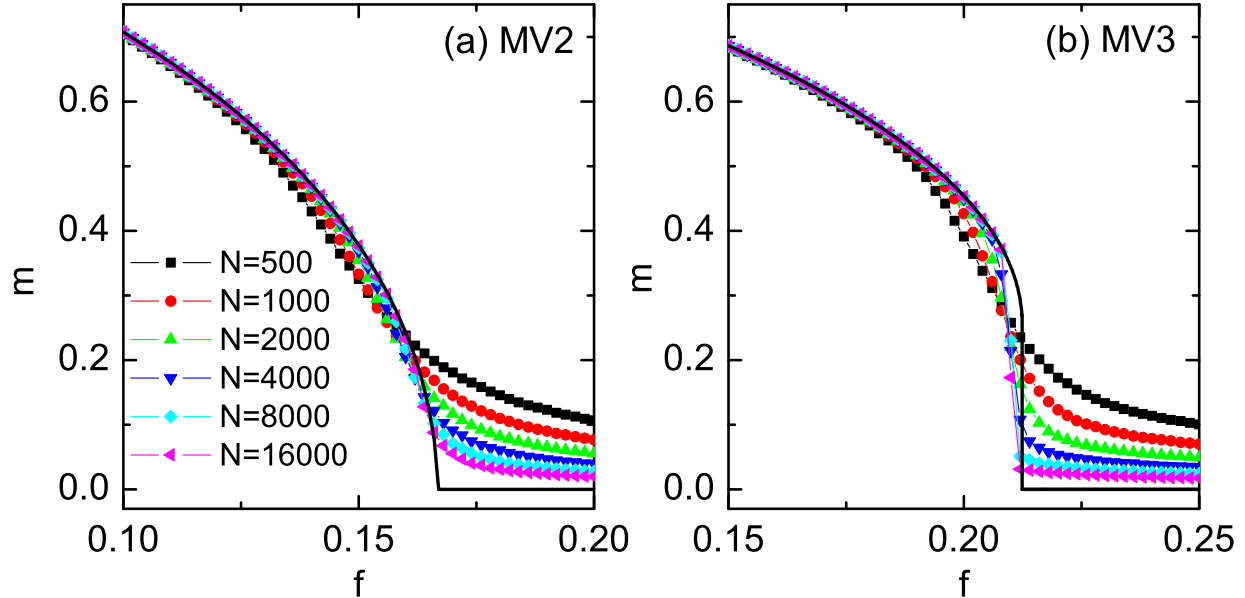


FIG. 1: (color online). Dependence of the order parameter m on the noise intensity f in the MV2 model (a) and in the MV3 model (b). The lines correspond to mean-field results.

III. SIMULATION RESULTS

We have performed extensive Monte Carlo (MC) simulation with various systems of size $N = 500, 1000, 2000, 4000, 8000, 16000$. At each elementary step, an agent is randomly chosen and tried to update its state according to its neighboring agents as defined before. Here, the neighboring agents are selected randomly from all other agents and the number of neighboring agents is fixed at $z = 4$. On each MC step (MCS), each agent is tried to update its state once on average. To obtain steady values of m , the first 10^5 MCS are discarded and the following 10^5 MCS are used to calculate time averages of m . At the critical region, larger runs are performed with 2×10^5 MCS to reach the steady state and 10^6 for computing time averages.

In Fig.1(a) and Fig.1(b), we show m as a function of the noise intensity f in the MV2 model and in the MV3 model, respectively. For the MV2 model, one can clearly see that the model displays a continuous order-disorder phase transition as the noise intensity f increases. The maximum in the susceptibility χ indicates that there exists an effective transition noise $f_c(N)$ for a given N , as shown in Fig.2(a). $f_c(N)$ increases with N and such a scaling determines a critical exponent of the continuous phase transition. For the MV3

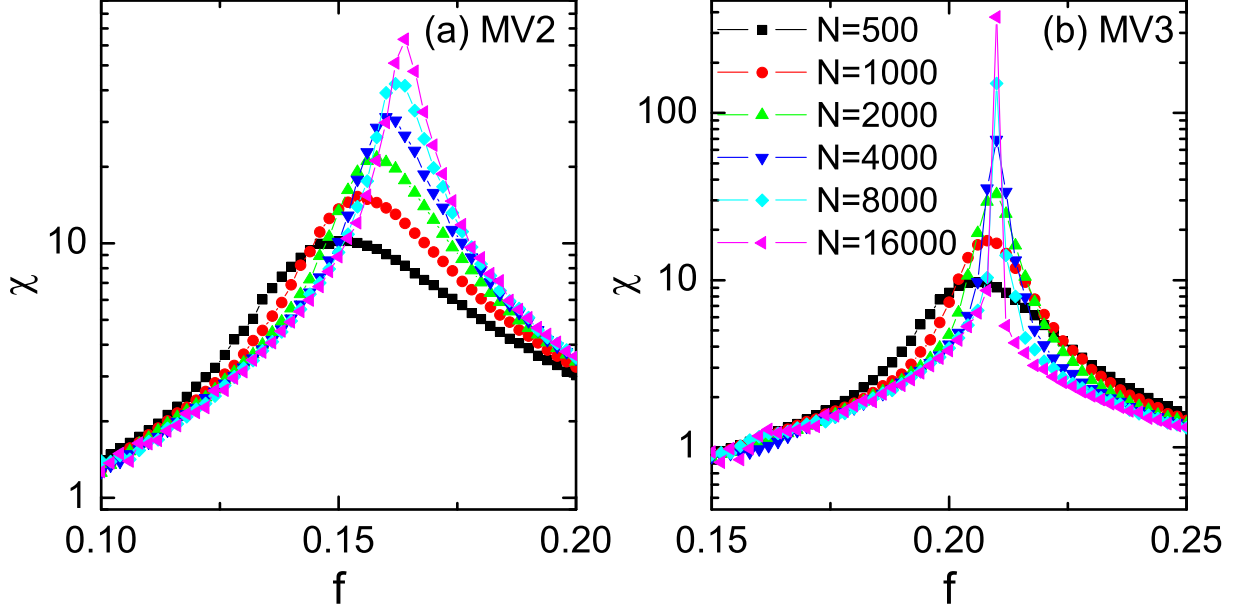


FIG. 2: (color online). Dependence of the susceptibility χ on the noise intensity f in the MV2 model (a) and in the MV3 model (b).

model, especially for a larger N , we find that m displays a sharp change close order-disorder phase transition. On the other hand, as shown in Fig.2(b), The susceptibility χ also shows a maximum at $f_c(N)$ but the change of χ near $f_c(N)$ becomes sharper and the values of χ at $f_c(N)$ becomes larger. These results may suggest the nature of phase transition in the MV3 model is different from that of the MV2 model.

To verify our hypothesis, we compare the results of the Binder's cumulant U in the MV2 model and in the MV3 model. For the MV2 model, the phase transition is continuous and the cumulants for different N intercept each other at $f = f_c^{MV2}$, providing a convenient estimate for the value of the critical noise $f_c^{MV2} \simeq 0.166$, as shown in Fig.3(a). In Fig.3(b), we plot the curves $U \sim f$ for different N in the MV3 model. In contrast to the case in MV2 model, U exhibits a nonmonotonic dependence on f and there exists a minimum near the onset of phase transition. For larger N , U falls to negative values near phase transition that is the sign of a discontinuous transition, together with the coexistence of the ordered and disordered phases expected then [25].

To further validate the discontinuous nature of phase transition in the MV3 model, in Fig.4 we plot a long time series of m close the transition noise for $N = 16,000$. It is clearly observed that the system flips between the ordered phase and disordered phase due to the

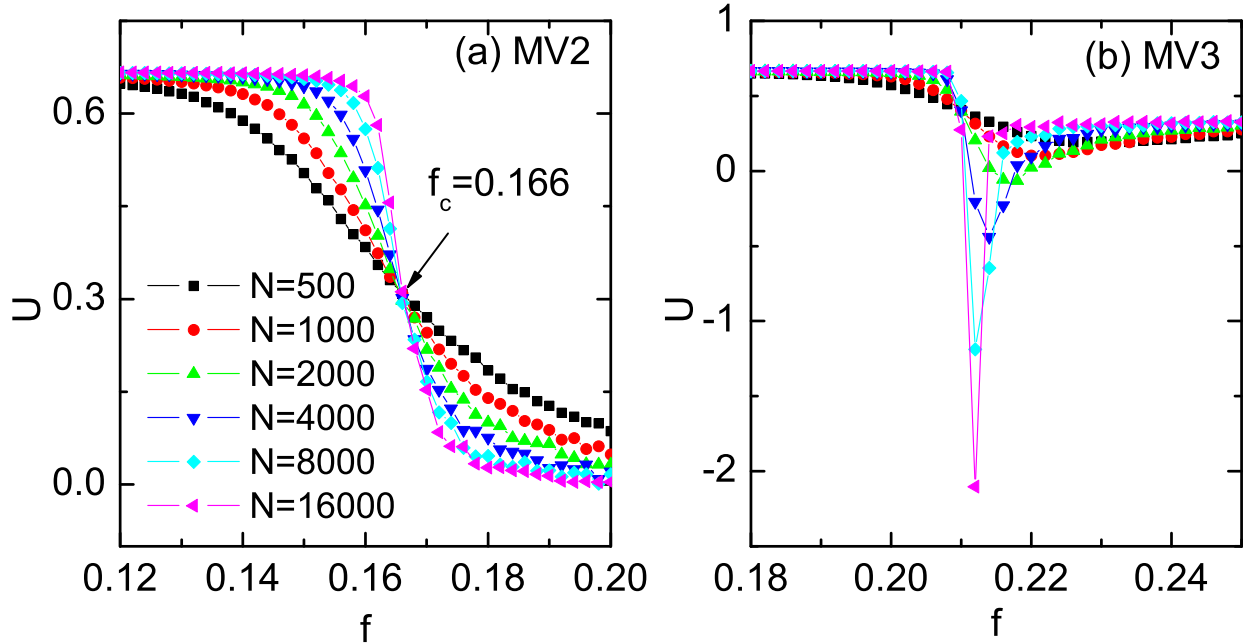


FIG. 3: (color online). Dependence of the Binder's fourth-order cumulant U on the noise intensity f in the MV2 model (a) and in the MV3 model (b).

finite-size fluctuations. This implies that at this noise the system is in the coexistence of the ordered and disordered phases, that is a typical of discontinuous phase transition. In Fig.5, we show the distribution of the values of m for several distinct values of f across the phase transition in the MV3 model for $N = 16,000$. For $f = 0.209$ (Fig.5(a)), m has a unique maximum around $m = 0.36$, which corresponds to an ordered phase. For $f = 0.2098$ (Fig.5(b)), m displays two peaks around $m = 0$ and $m = 0.34$ which indicate the coexistence of an ordered phase and a disordered one. Upon increasing the value of f , the peak at $m = 0$ is enhanced, while the other peak is depressed (see Fig.5(c) for $f = 0.2102$), implying that the disorder phase becomes more stable. For even larger values of f , there remains a single peak around $m = 0$, which indicates that the system is in a disordered phase (see Fig.5(d) for $f = 0.211$). This set of histograms further verify that the MV3 model undergoes a discontinuous order-disorder transition. Note that if the network configuration among agents is quenched other than annealed used in the present work, the MV3 also displays a continuous phase transition as in the MV2 model [22].

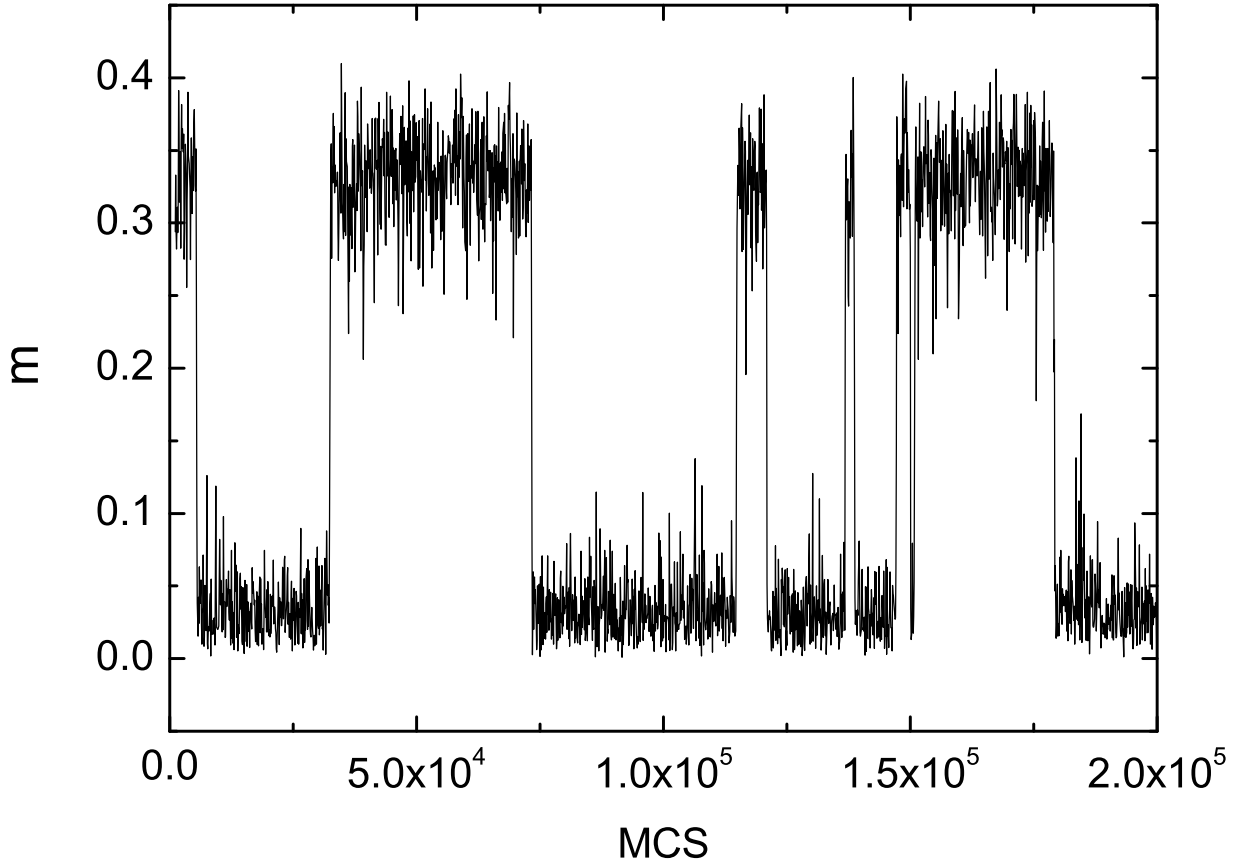


FIG. 4: A long time series of order parameter m close the phase transition in the MV3 model. The parameters are $f = 0.21$ and $N = 16,000$.

IV. MEAN-FIELD THEORY

To analytical understand the difference on the nature of phase transitions between the MV2 model and the MV3 model, we will present a mean-field theory to determine steady values of m as a function of f . To the end, let x_α denote the probability that each node is in the state α ($\alpha = 1, \dots, q$). The time evolution of x_α can be written as

$$\dot{x}_\alpha = \sum_{\beta \neq \alpha} x_\beta w_{\beta \rightarrow \alpha} - x_\alpha \sum_{\beta \neq \alpha} w_{\alpha \rightarrow \beta} \quad (4)$$

where $w_{\alpha \rightarrow \beta}$ is the transition rate from state α to state β . According to our model, the rate $w_{\alpha \rightarrow \beta}$ can be expressed as the sum of two parts,

$$w_{\alpha \rightarrow \beta} = (1 - f)P_\beta + f\tilde{P}_\beta \quad (5)$$

where the first part is the probability of taking majority-rule $1 - f$ by the probability P_β that the state β is in the majority state, and the second part is the probability of taking

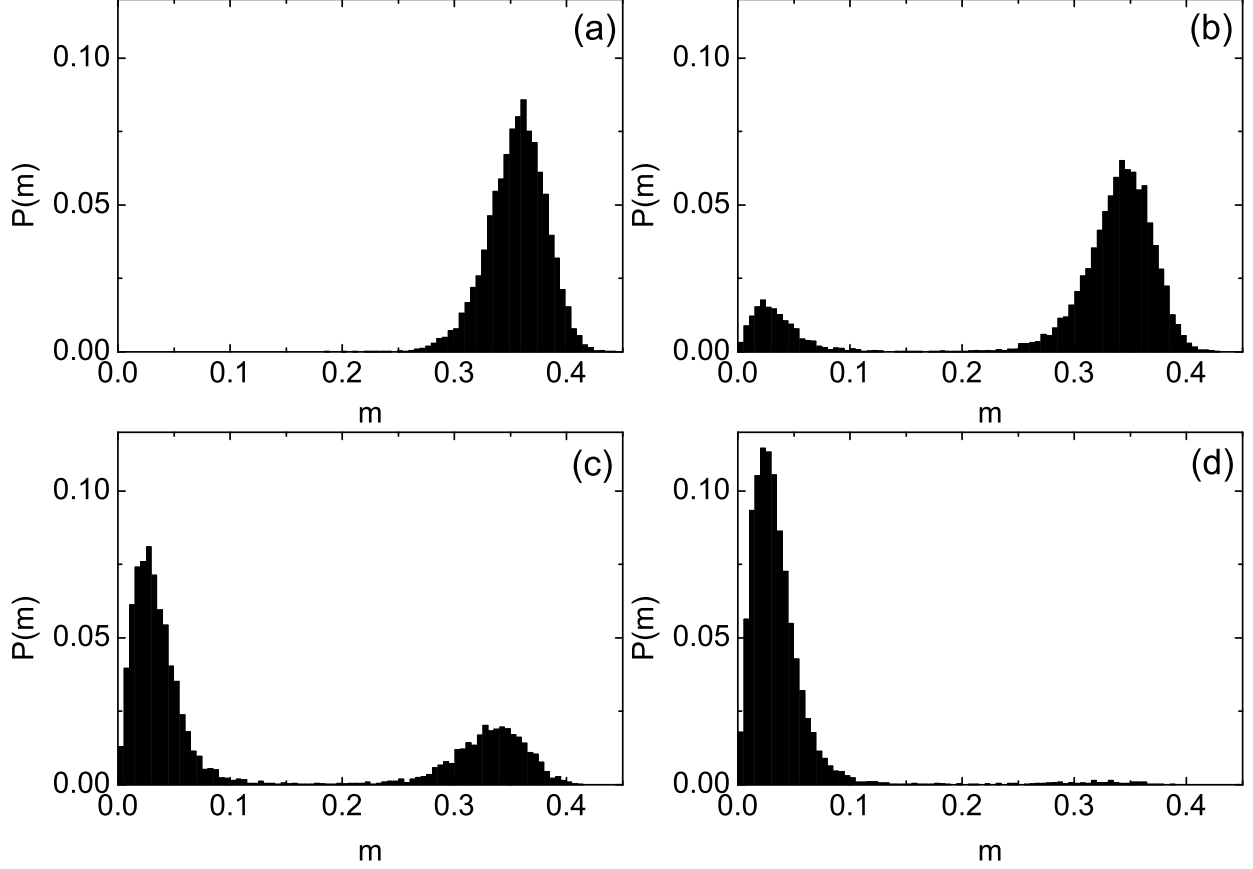


FIG. 5: Histogram of the values of order parameter m across a discontinuous phase transition in the MV3 model. The noise intensity f are 0.209, 0.2098, 0.2102, and 0.211 from (a) to (d), respectively. The size of the system is $N = 16,000$.

minority-rule f by the probability \tilde{P}_β that the state β is in the minority state. Using the normalization conditions, $\sum_\beta x_\beta = \sum_\beta P_\beta = \sum_\beta \tilde{P}_\beta = 1$, Eq.(4) can be simplified to

$$\dot{x}_\alpha = -x_\alpha + (1 - f)P_\alpha + f\tilde{P}_\alpha. \quad (6)$$

In the steady state $\dot{x}_\alpha = 0$, we have

$$x_\alpha = (1 - f)P_\alpha + f\tilde{P}_\alpha. \quad (7)$$

Let n_α denote the number of neighbors in the state α among all z neighbors, and the probability of a given configuration $\{n_\alpha\}$ can be written as multinomial distribution,

$$p(\{n_\alpha\}) = \frac{z!}{\prod_\alpha n_\alpha!} \prod_\alpha x_\alpha^{n_\alpha}. \quad (8)$$

Thus, P_α and \tilde{P}_α can be expressed as

$$P_\alpha = \sum_{\{n_\alpha\} | n_\alpha > n_\beta, \forall \beta \neq \alpha} p(\{n_\alpha\}) + \sum_{\{n_\alpha\} | n_\alpha = n_\beta > n_\gamma, \forall \gamma \neq \alpha, \beta} \frac{1}{2} p(\{n_\alpha\}) + \dots, \quad (9)$$

and

$$\tilde{P}_\alpha = \sum_{\{n_\alpha\} | n_\alpha < n_\beta, \forall \beta \neq \alpha} p(\{n_\alpha\}) + \sum_{\{n_\alpha\} | n_\alpha = n_\beta < n_\gamma, \forall \gamma \neq \alpha, \beta} \frac{1}{2} p(\{n_\alpha\}) + \dots, \quad (10)$$

In the present work, the number of neighbors of each agent is kept at $z = 4$. For the MV2 model, P_α and \tilde{P}_α are

$$\begin{cases} P_\alpha = x_\alpha^4 + 4x_\alpha^3 x_\beta + 3x_\alpha^2 x_\beta^2 \\ \tilde{P}_\alpha = x_\beta^4 + 4x_\alpha x_\beta^3 + 3x_\alpha^2 x_\beta^2 \end{cases}, \quad (11)$$

where $\alpha, \beta \in \{1, 2\}$ and $\alpha \neq \beta$. One can easily check that $x_\alpha = \frac{1}{2}$ ($\alpha = 1, 2$) is always a set of solution of Eq.(4) for any given f . This trivial solution corresponds to a disordered phase. The solution loses its stability when the maximal eigenvalue of Jacobi matrix is larger than zero, which leads to the analytical value of the critical noise $f_c^{MV2} = \frac{1}{6}$. The other solutions can be obtained by numerically solving Eq.(7) combined with Eq.(11). In Fig.6(a), we show the steady solutions of m as a function of f . The solid and dashed lines indicate the stable and the unstable steady solutions, respectively. The MV2 model presents a continuous order-disorder phase transition at $f = f_c^{MV2} = \frac{1}{6}$.

For MV3 model, P_α and \tilde{P}_α are

$$\begin{cases} P_\alpha = x_\alpha^4 + 4x_\alpha^3 x_\beta + 4x_\alpha^3 x_\gamma + 3x_\alpha^2 x_\beta^2 + 3x_\alpha^2 x_\gamma^2 + 12x_\alpha^2 x_\beta x_\gamma \\ \tilde{P}_\alpha = \frac{1}{2}x_\beta^4 + \frac{1}{2}x_\gamma^4 + 4x_\beta^3 x_\gamma + 4x_\beta x_\gamma^3 + 6x_\beta^2 x_\gamma^2 + 6x_\alpha x_\beta^2 x_\gamma + 6x_\alpha x_\beta x_\gamma^2 \end{cases} \quad (12)$$

where $\alpha, \beta, \gamma \in \{1, 2, 3\}$ and $\alpha \neq \beta \neq \gamma$. Since $P_\alpha = \tilde{P}_\alpha = \frac{1}{3}$ at $x_\alpha = \frac{1}{3}$ ($\alpha = 1, 2, 3$) (corresponding to a disordered phase), one can easily check that Eq.(4) holds for any given f . As mentioned before, this trivial solution loses its stability when the maximal eigenvalue of Jacobi matrix is larger than zero. It immediately leads to the analytical value of $f_{c1}^{MV3} = \frac{15}{78} \simeq 0.1923$. The other solutions can be obtained by numerically solving Eq.(7) combining with Eq.(12). In Fig.6(b), we show the steady solutions of m as a function of f . The solid line, dashed line and dotted line correspond that the solutions are stable, unstable and saddle, respectively. As f varies forward and backward, m presents two discontinuous

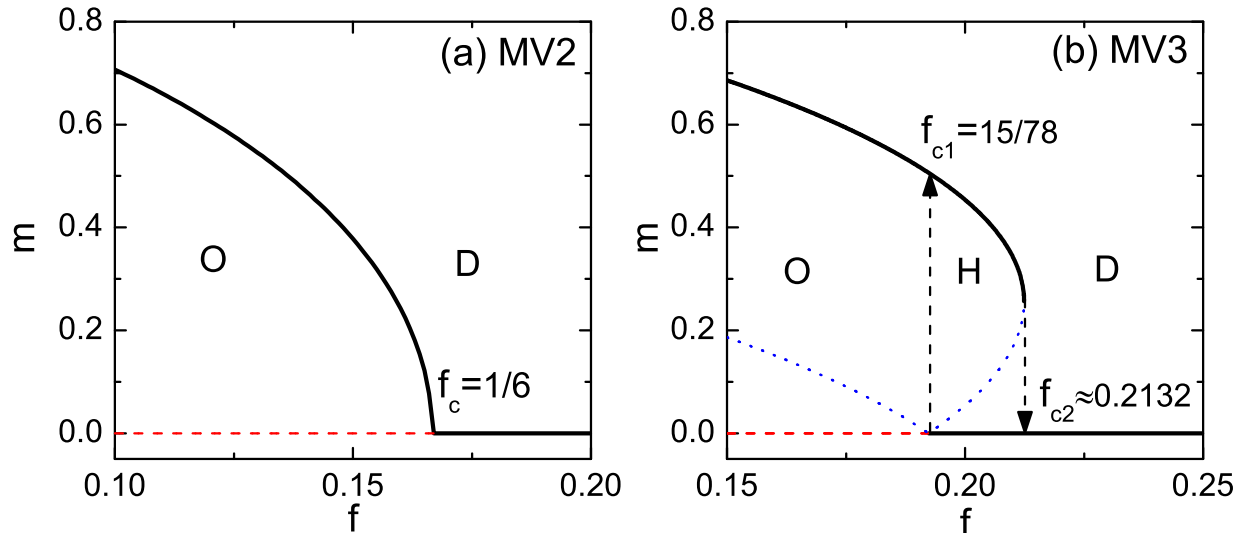


FIG. 6: (color online). The steady solutions of m in the MV2 model (a) and in the MV3 model (b). The MV2 model displays a continuous order-disorder (O-D) phase transition at $f = f_c^{MV2} = \frac{1}{6}$. The MV3 model displays a discontinuous O-D phase transition at $f = f_c^{MV3} \simeq 0.2132$ and a discontinuous D-O phase transition at $f = f_{c1}^{MV3} = \frac{15}{78}$ as f varies forward and backward. In the hysteresis (H) region between f_{c1}^{MV3} and f_{c2}^{MV3} , the MV3 model is in the coexistence of O phase and D phase. The solid line, dashed line and dotted line correspond that the solutions are stable, unstable and saddle, respectively.

transitions at $f = f_{c2}^{MV3} \simeq 0.2132$ and at $f = f_{c1}^{MV3}$. This indicates that there exists a hysteresis region at $f_{c1}^{MV3} < f < f_{c2}^{MV3}$ for which the ordered phase and disordered phase are coexisting.

V. CONCLUSIONS AND DISCUSSION

In conclusion, we have generalized the original MV model from two states to arbitrary multiple states. We have made the detailed comparison on the nature of phase transitions between the MV2 model and the MV3 model defined on annealed networks. Interestingly, we have found that the discontinuous nature of order-disorder phase transition in the MV3 model, qualitatively different from the continuous phase transition in the MV2 model. By a mean-field analysis, we have obtained the steady solutions of order parameter m as a function of noise f . Based on the stability analysis of the solutions, we have obtained

the analytical value $f_{c_2}^{MV3}$ of noise for the onset of the discontinuous disorder-order phase transition. Another value $f_{c_1}^{MV3}$ of noise for the onset of the discontinuous order-disorder phase transition is also numerically estimated. In the hysteresis region between these two transition noises, the MV3 model is coexistent of an ordered phase and a disordered one. For a finite size system, the fluctuation can drive the flips between these two phases. Our findings may suggest a novel mechanism of first-order phase transitions in nonequilibrium systems. At last, we should emphasize that there exists the essential difference in the nature of phase transition between the annealed and quenched MV3 models [22].

Acknowledgments

This work was supported by National Science Foundation of China (Grants Nos. 11205002, 61473001, 11475003, 11405001), the Key Scientific Research Fund of Anhui Provincial Education Department (Grant No. KJ2016A015) and “211” Project of Anhui University (Grant No. J01005106).

-
- [1] D. Stauffer, *Am. J. Phys.* **76**, 470 (2008).
 - [2] C. Castellano, S. Fortunato, and V. Loreto, *Rev. Mod. Phys.* **81**, 591 (2009).
 - [3] M. J. de Oliveira, *J. Stat. Phys.* **66**, 273 (1992).
 - [4] W. Kwak, J.-S. Yang, J.-i. Sohn, and I.-m. Kim, *Phys. Rev. E* **75**, 061110 (2007).
 - [5] Z.-X. Wu and P. Holme, *Phys. Rev. E* **81**, 011133 (2010).
 - [6] A. L. Acuña Lara, F. Sastre, and J. R. Vargas-Arriola, *Phys. Rev. E* **89**, 052109 (2014).
 - [7] A. L. Acuña Lara and F. Sastre, *Phys. Rev. E* **86**, 041123 (2012).
 - [8] G. Grinstein, C. Jayaprakash, and Y. He, *Phys. Rev. Lett.* **55**, 2527 (1985).
 - [9] L. F. C. Pereira and F. G. B. Moreira, *Phys. Rev. E* **71**, 016123 (2005).
 - [10] F. W. S. Lima, A. Sousa, and M. Sumuor, *Physica A* **387**, 3503 (2008).
 - [11] P. R. A. Campos, V. M. de Oliveira, and F. G. B. Moreira, *Phys. Rev. E* **67**, 026104 (2003).
 - [12] E. M. S. Luz and F. W. S. Lima, *Int. J. Mod. Phys. C* **18**, 1251 (2007).
 - [13] T. E. Stone and S. R. McKay, *Physica A* **419**, 437 (2015).
 - [14] F. W. S. Lima, *Int. J. Mod. Phys. C* **17**, 1257 (2006).

- [15] F. W. S. Lima and K. Malarz, *Int. J. Mod. Phys. C* **17**, 1273 (2006).
- [16] H. Chen, C. Shen, G. He, H. Zhang, and Z. Hou, *Phys. Rev. E* **91**, 022816 (2015).
- [17] J.-S. Yang, I.-m. Kim, and W. Kwak, *Phys. Rev. E* **77**, 051122 (2008).
- [18] J. Santos, F. Lima, and K. Malarz, *Physica A* **390**, 359 (2011).
- [19] A. Brunstein and T. Tomé, *Phys. Rev. E* **60**, 3666 (1999).
- [20] T. Tomé and A. Petri, *J. Phys. A* **35**, 5379 (2002).
- [21] F. Y. Wu, *Rev. Mod. Phys.* **54**, 235 (1982).
- [22] D. F. F. Melo, L. F. C. Pereira, and F. G. B. Moreira, *J. Stat. Mech.* p. P11032 (2010).
- [23] F. Lima, *Physica A* **391**, 1753 (2012).
- [24] L. S. A. Costa and A. J. F. de Souza, *Phys. Rev. E* **71**, 056124 (2005).
- [25] K. Binder, *Rep. Prog. Phys.* **60**, 487 (1997).